NUCLEAR THEORY, Vol. 39 (2022)
eds. M. Gaidarov, N. Minkov, Heron Press, Sofia

Prediction of Monte Carlo Event Generator to Probe the Shower Implementation

Nameeqa Firdous[1], **Malik Muhammad Junaid**[2]

[1]GIFT University, Gujranwala, Pakistan
[2]University of Innsbruck, Innsbruck, Austria

Abstract. To understand high-energy collisions in a better way, a detailed simulation of collision events is needed which is provided by General-purpose Monte Carlo generators . They are considered as an indispensable tool in QCD modelling, data analysis and planning the new experiments. They are used together with detector simulation to estimate signals and backgrounds in high-energy processes. The generators used for this study are PYTHIA8, a parton based generator and it simulates parton interactions and parton showers, where the hadronization is treated using the Lund string fragmentation model. In this study we will investigate the shower implementation of PYTHIA8.3. There are three different complete parton-shower frameworks introduced : the original simple showers, the VINCIA antenna showers and the Dire dipole showers. Comparisons between these different shower approaches are presented using best fit to the Minimum bias data from the ATLAS experiment at 7 TeV. Simple Shower is the old shower framework and is a default choice that has its roots in PYTHIA 6, and studies show this model is more mature and stable as compared to the other two options.

1 Introduction

PYTHIA is a highly successful and well established Monte Carlo event generator [1,2], and developed extensively in the last decades. It can describe most of the experimental data/observables quite well as compared to other event generators. It is based on a phenomenological adaptation of Quantum chromodynamics to describe hadronic interactions, especially soft interactions where low momentum transfer is involved. This is done by introducing several phenomenological models for all physics processes like Multiparton interactions (MPI), initial and final state radiations (ISR, FSR) and hadronization etc. These models have free parameters which need to be tuned to describe the experimental data [3].

Frameworks that will be used in a run are determined by the following switch [4]:

mode PartonShowers:model (default = 1; minimum = 1; maximum = 3)

For the selection of shower models PYTHIA8.3 has introduced three different complete parton-shower frameworks: simple showers also known as timelike/Space-like showers, the VINCIA antenna showers and the Dire dipole showers. In the older version of PYTHIA 8 external shower programs can be linked by replacing the internal default one. The VINCIA and Dire codes originally were developed and distributed as separate codes to be linked if required by the user. Starting with version 8.3, these two programs now are fully incorporated into the PYTHIA software, as the default option simple showers. The selection of all three internal showers implemented in PYTHIA 8 can be done as follows:.

Option 1: Simple Showers. This is the old shower framework that has its roots in PYTHIA 6 and has been distributed with PYTHIA 8 since the beginning. It is a more mature and stable model option as compared two other two new shower options, that's why it for now remains as default. It also has some special features that the other two don't.

Option 2: VINCIA Showers. it is based on sequences of pT-ordered 23 branchings, the VINCIA shower model is similar to that of ARIADNE, which it resembles strongly for final-state evolution while VINCIA adopts a different picture for initial-state radiation termed as backwards evolution. The branching kernels, known as antenna functions, treat coherent sums of parton pairs without requiring a separation into radiators and spectators. The current PYTHIA implementation includes QCD and QED 23 branchings with full mass dependence and, for the latter, multipole interference effects.

Option 3: Dire Showers [5] (Dipole resummation). Dire implements a transverse-momentum ordered dipole shower in which radiator-spectator particle pairs evolve simultaneously. The emission phase space is fully symmetric between radiator and spectator, while the overall emission probability is separated into two pieces that are enhanced (suppressed) in region collinear (anti-collinear) to the radiator or the spectator, respectively. Dire includes QCD and QED emissions, a detailed treatment of (quark/lepton) mass effects, and is set up to include higher-order corrections, such as triple-collinear or double-soft parton emissions.

For the better understanding of high energy hadronic interactions or to search for new physics phenomena at hadron colliders, it is crucial to have a good understanding of the hard scattering process along with the accompanying interactions of the rest of the proton-proton collision termed as the underlying event (UE). As the UE is an integral part of the same proton-proton collision, accurate description of its properties by Monte Carlo (MC) event generators is important for the LHC physics programme. Modelling of UE can receive contributions from initial- and final-state radiation (ISR, FSR), from the QCD evolution of colour connections between the hard scattering and the beam-proton remnants, and also multiple partonic interactions (MPI). As it is significantly influenced by physics not currently calculable from first principles, the measurement of the UEs properties is crucial not only for better understanding of the mechanisms involved but also to provide input for tuning of the free parameters of phenomenological UE models in MC event generators. Although the underlying event cannot be separated from the hard scattering process, observables can be defined which are particularly sensitive to the properties of the UE [6].

2 Definition of Underlying-Event Observables

The data used in this study is underlying event data at 7 TeV from ATLAS Collaboration. This data uses the established form of UE observables [7], in which the azimuthal plane of the event is separated into several distinct regions with differing sensitivities to the UE. As illustrated in Figure 1, the azimuthal angular difference with respect to the leading (highest-pT) charged particle $|\Delta\varphi| = |\varphi - \varphi \text{ lead}|$, is used to define the regions:

- $|\Delta\varphi| < 60°$, the towards region;
- $60° < |\Delta\varphi| < 120°$, the transverse region; and
- $|\Delta\ \varphi| > 120°$, the away region.

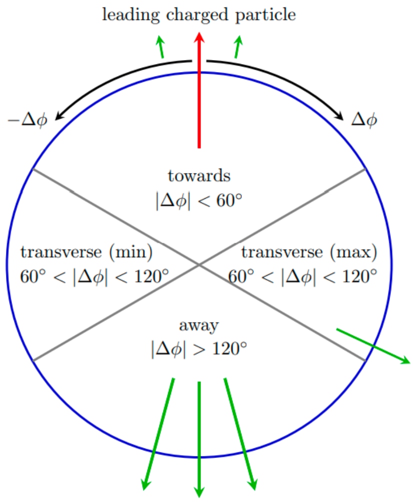

Figure 1. Definition of regions in the azimuthal angle with respect to the leading (highest-pT) charged particle, with arrows representing particles associated with the hard scattering process [6].

3 Results

The list of sensitive observables of underlying event and Minimum Bias events are given in Table 1 and Table 2, respectively at 7 TeV. Comparison between MC and Minimum Bias data is given in Figure 2. It is shown that eta distribution is better described by simple shower option where VINCIA underestimates and

Table 1. List of observables of minimum bias event data at 7 TeV [8]

Observable	ATLAS minimum bias event data	ECM
Nch	Track Pt $>$ 500 MeV, Nch $\geq$ 1	0.9 TeV
Pt	Track Pt $>$ 500 MeV, Nch $\geq$ 1	0.9 TeV
Eta	Track Pt $>$ 500 MeV, Nch $\geq$ 1	0.9 TeV
$\langle$Pt$\rangle$ vs Nch	Track Pt $>$ 500 MeV, Nch $\geq$ 1	0.9 TeV
Nch	Track Pt $>$ 500 MeV, Nch $\geq$ 6 (diffraction suppressed)	0.9 TeV
Pt	Track Pt $>$ 500 MeV, Nch $\geq$ 6 (diffraction suppressed)	0.9 TeV
Eta	Track Pt $>$ 500 MeV, Nch $\geq$ 6 (diffraction suppressed)	0.9 TeV
Nch	Track Pt $>$ 500 MeV, Nch $\geq$ 1	7 TeV
Pt	Track Pt $>$ 500 MeV, Nch $\geq$ 1	7 TeV
Eta	Track Pt $>$ 500 MeV, Nch $\geq$ 1	7 TeV
$\langle$Pt$\rangle$ vs Nch	Track Pt $>$ 500 MeV, Nch $\geq$ 1	7 TeV
Nch	Track Pt $>$ 500 MeV, Nch $\geq$ 6 (diffraction suppressed)	7 TeV
Pt	Track Pt $>$ 500 MeV, Nch $\geq$ 6 (diffraction suppressed)	7 TeV
Eta	Track Pt $>$ 500 MeV, Nch $\geq$ 6 (diffraction suppressed)	7 TeV

Table 2. List of observables of underlying event data at 7 TeV [9]

Observable, ATLAS underlying event data	ECM
Transverse region Nch density vs pT (leading track)	0.9 TeV
Toward region Nch density vs pT (leading track)	0.9 TeV
Away region Nch density vs pT (leading track)	0.9 TeV
Transverse region ΣpT density vs pT (leading track)	0.9 TeV
Toward region ΣpT density vs pT (leading track)	0.9 TeV
Away region ΣpT density vs pT (leading track)	0.9 TeV
Transverse region density vs pT (leading track)	0.9 TeV
Toward region density vs pT (leading track)	0.9 TeV
Away region density vs pT (leading track)	0.9 TeV
Transverse region density vs Nch	0.9 TeV
Toward region density vs Nch	0.9 TeV
Away region density vs Nch	0.9TeV
Transverse region Nch density vs pT (leading track)	7 TeV
Toward region Nch density vs pT (leading track)	7 TeV
Away region Nch density vs pT (leading track)	7 TeV
Transverse region ΣpT density vs pT (leading track)	7 TeV
Toward region ΣpT density vs pT (leading track)	7 TeV
Away region ΣpT density vs pT (leading track)	7 TeV
Transverse region density vs pT (leading track)	7 TeV
Toward region density vs pT (leading track)	7 TeV
Away region density vs pT (leading track)	7 TeV
Transverse region density vs Nch	7 TeV
Toward region density vs Nch	7 TeV
Away region density vs Nch	7 TeV

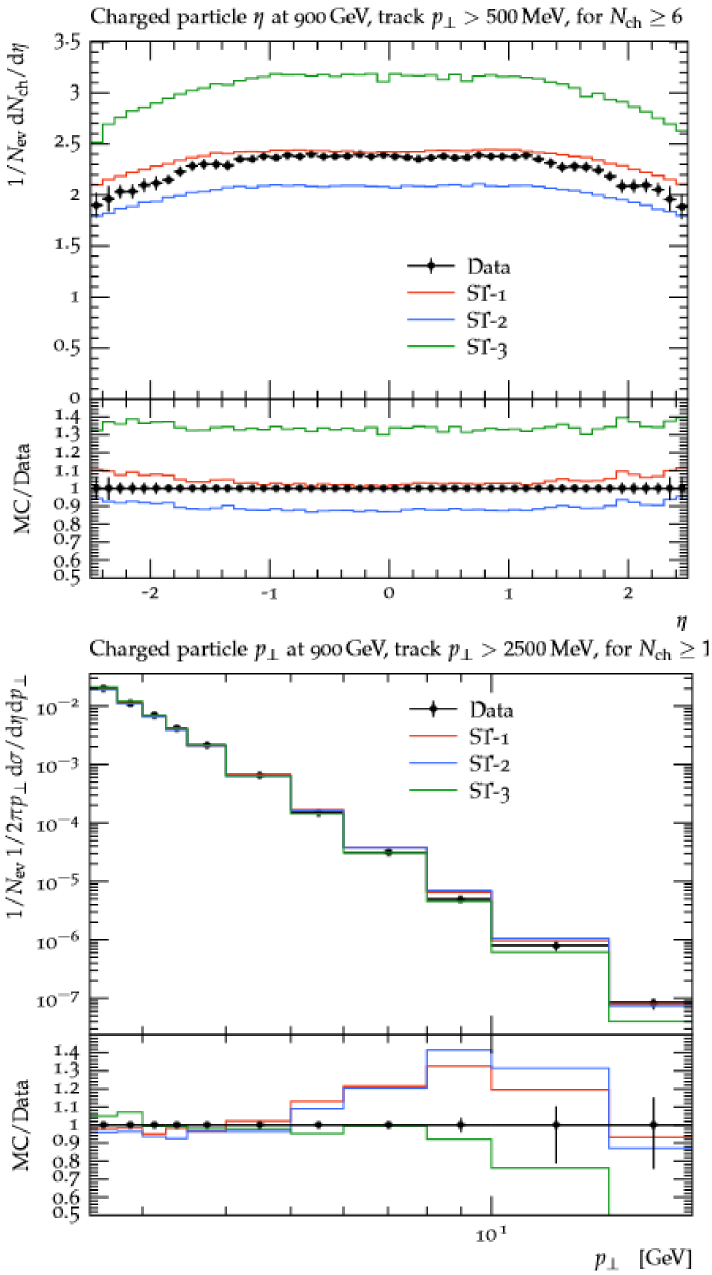

Figure 2. Data / MC comparison plots of eta and pt distributions at 7 TeV.

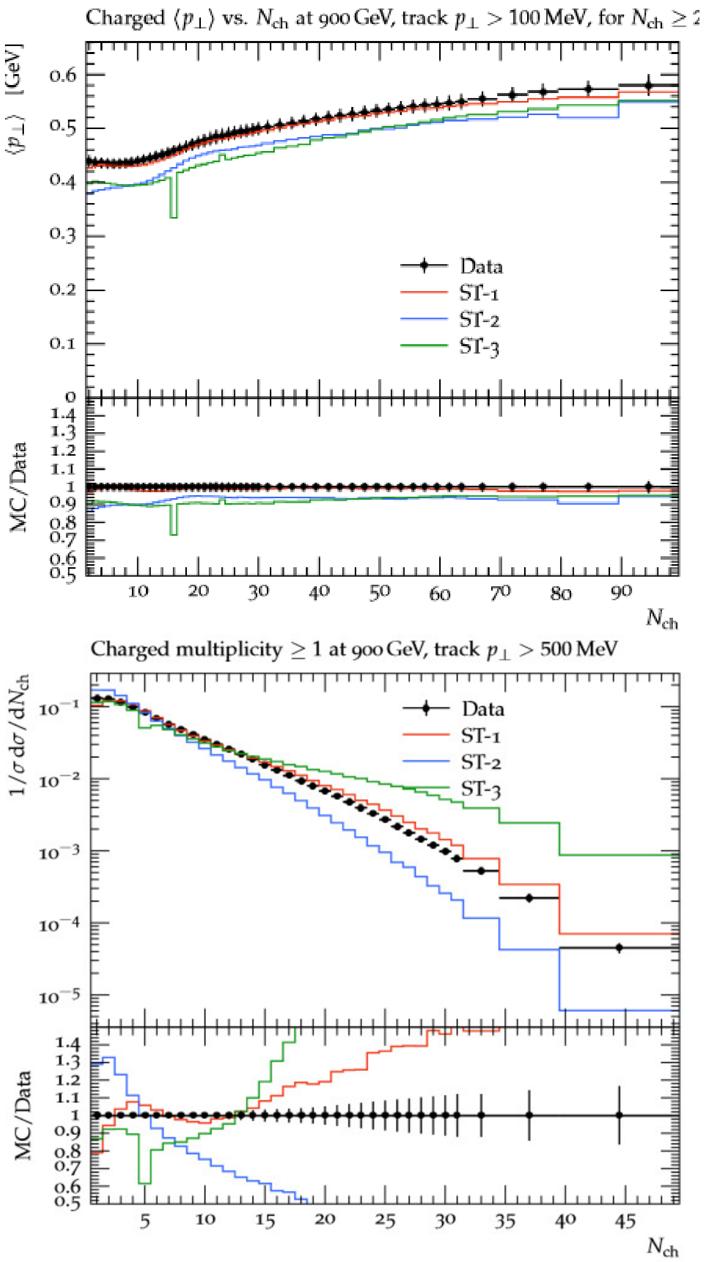

Figure 3. Data / MC comparison plots of Eta and charged particle multiplicity distributions at 7 TeV.

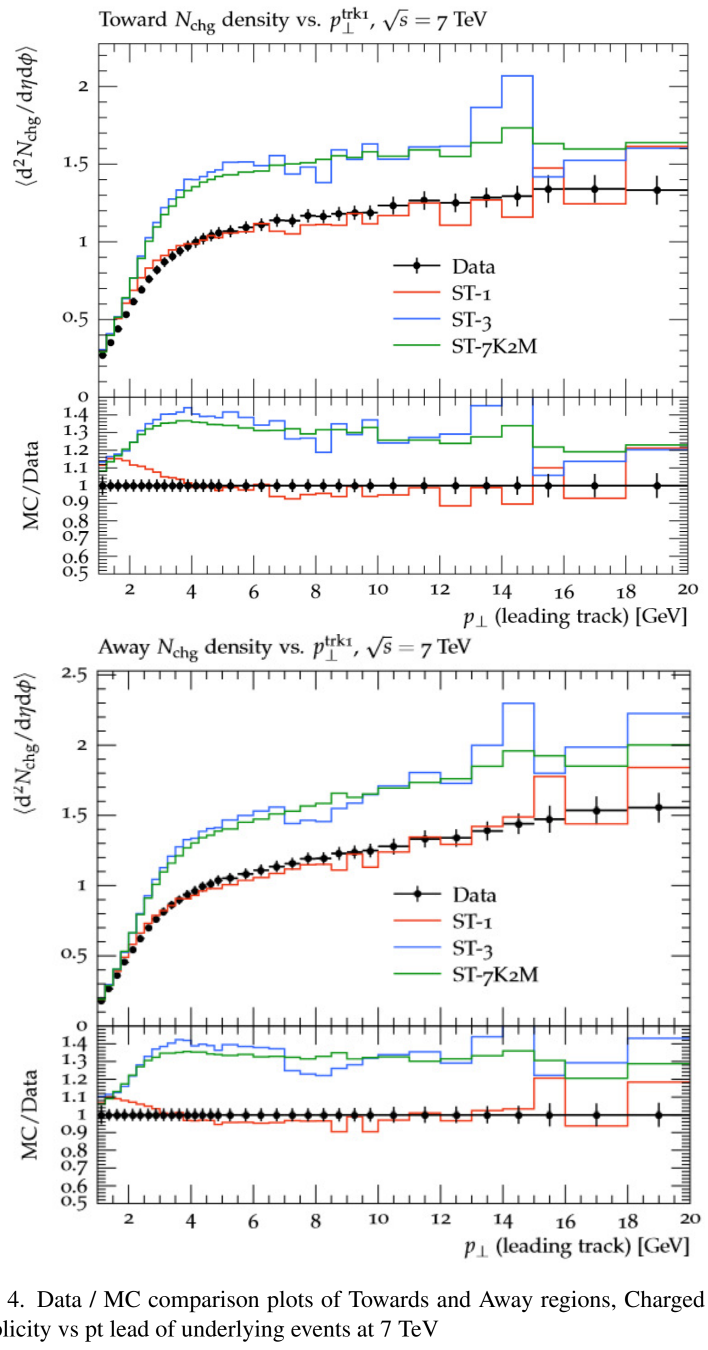

Figure 4. Data / MC comparison plots of Towards and Away regions, Charged particle Multiplicity vs pt lead of underlying events at 7 TeV

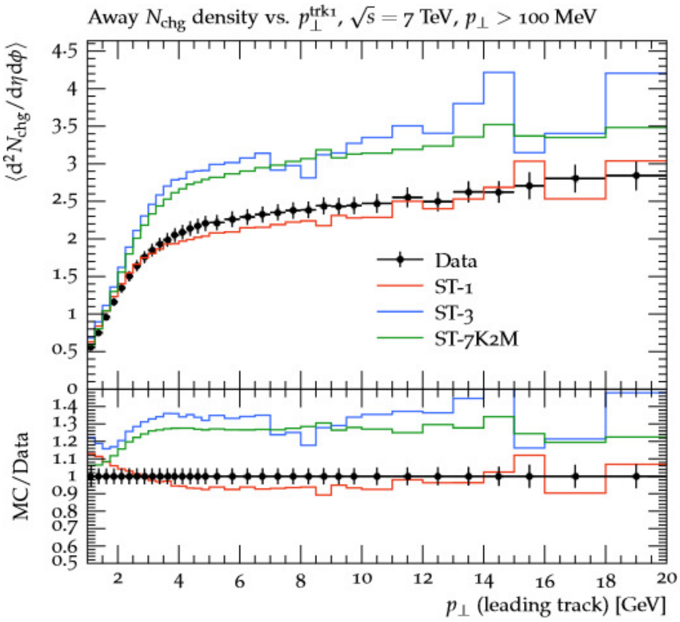

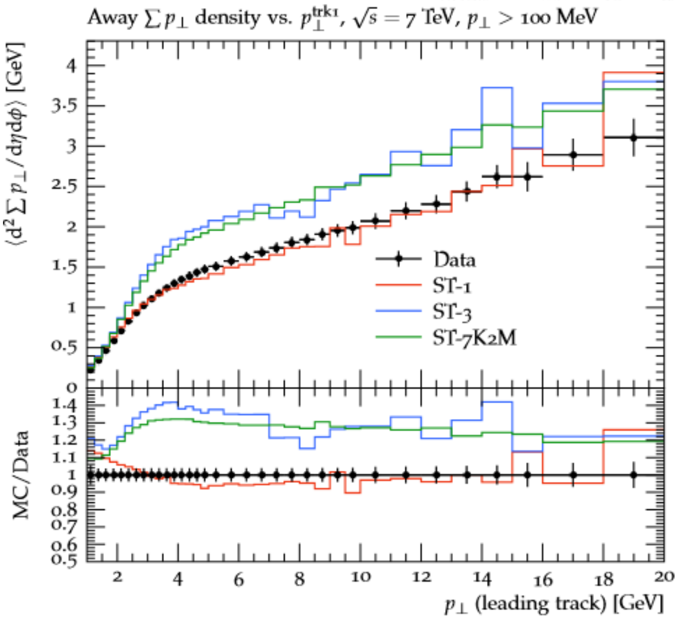

Figure 5. Data / MC comparison plots of Towards and Away regions, sumPt vs pt lead of underlying events at 7 TeV

Dire overestimates the data. Situation is quite better for the Pt distribution as all the three shower options describe data in the same manner, descrepancy is seen at higher pt but it is not very significant. Figure 3 shows average pt vs charged particle multiplicity, this onservable is better described by simple shower where other showers need more activity. The comparison between charged particle multiplicity density and MC generated for three different shower options is shown in Figure 4 as a function of pt lead at 7 TeV. For the 7 TeV data, the average number of charged particles in the transverse region doubles in going from p lead T = 2 to 5 GeV, and then forms an approximately constant plateau for p lead T $>$ 5 GeV. Data was well described by option 1 i.e, simple model as compared to other two shower options in transverse, towards and away regions as defined above in section 2. Dire and VINCIA show more activity as required by data and overestimate the data. This behavior is clearly seen in other observables in Figure 5, which shows comparison of the average charged particle pT as a function of ptlead data and MC generated by three shower options in towards and away regions. Figure 4 shows the data-MC comparison of the mean pT of charged particles and the charged particle multiplicity in each region is sensitive to the amount of hard (perturbative QCD) versus soft (non-perturbative QCD) processes contributing to the UE. These distributions are relatively well defined by all three shower options.

4 Conclusion

We have presented effects of different shower options on the sensitive observables of Minimum Bias and Underlying events, measured by the ATLAS experiment at the 7 TeV. The measured observables are defined using charged tracks. For the selected observables each event is azimuthally segmented into three regions with respect to the highest-pT charged particle. The three regions are named as towards, transverse, and away. All the three shower approaches describe data with some differences. Simple shower approach provides the best results as this model is more mature as compared to other two approaches which need detailed study [11] and tuning as well. This study is done with the default settings and agreement between MC and experimental data can be further improved by tuning the free parameters of the selected models. All plots used in this study are produced using Rivet toolkit [10].

References

[1] M. Seymour, M. Marx, https://arxiv.org/abs/1304.6677.

[2] A. Buckley, H. Hoeth, H. Lacker, H.,Schulz, J. Seggern, *Eur. Phys. J. C* **65** (2009) 331-357.

[3] N. Firdous, G. Rudolph, *EPJ Web of Conferences*. **60** (2013) 20056.

[4] C. Bierlich, S. Chakraborty, N. Desai, L. Gellersen, I. Helenius, P. Ilten, L., Lönnblad, S. Mrenna, S. Prestel, C. Preuss, T. Sjöstrand, P. Skands, M. Utheim, R. Verheyen, https://arxiv.org/abs/2203.11601.

[5] S. Höche, S. Prestel, *Eur. Phys. J. C* **75**(2015) 461.
[6] M. Aaboud, G. Aad, et al. (ATLAS Collaboration), *J. High Ener. Phys.* **2017** (2017) 157.
[7] Y. Kulchitsky, https://arxiv.org/abs/1608.04954.
[8] G. Aad et al. (ATLAS Collaboration), *Phys. Rev. D* **83** (2011) 112001.
[9] G. Aad et al., *New J. Phys.* **13** (2011) 053033.
[10] C. Bierlich, et al., *SciPost Phys.* **8** (2020) 026.
[11] N. Firdous, G. Rudolph, *EPJ Web of Conferences*. **60** (2013) 20009.